Available online at www.sciencedirect.com
SCIENCE DIRECT®
Journal of Nuclear Materials 342 (2005) 20–25
journal of nuclear materials
www.elsevier.com/locate/jnucmat

Limitations of W and W–1%La_2O_3 for use as structural materials

Michael Rieth [a,*], Bernhard Dafferner [b]

[a] Forschungszentrum Karlsruhe, Institut für Materialforschung I, P.O. Box 3640, 76021 Karlsruhe, Germany
[b] Forschungszentrum Karlsruhe, Institut für Materialforschung II, P.O. Box 3640, 76021 Karlsruhe, Germany

Received 2 March 2005; accepted 18 March 2005

Abstract

Recent divertor designs for future fusion demonstration reactors include dispersion strengthened tungsten as structural material. Their operation temperature window – currently estimated to be between 800 °C and 1200 °C – is restricted by embrittlement on the lower limit. Therefore, standard impact tests have been performed with specimens fabricated from commercial tungsten and W–1%La_2O_3 rods. Due to the anisotropic microstructure, specimens were oriented parallel to rod axis for optimum Charpy properties. Nevertheless, ductile-to-brittle transition temperatures of just 800 ± 50 °C for tungsten and approximately 950 ± 50 °C for W–1%La_2O_3 have been determined. But for use as structural material under fusion-specific neutron irradiation, an according alloy should exhibit transition temperatures of 200–400 °C, at least. Therefore, the impact of these results on the use of dispersion strengthened tungsten for divertor structures are discussed in detail.

1. Introduction

In the future fusion demonstration reactor DEMO the divertor has to withstand very high heat fluxes in the order of 10–15 MW/m^2 and has to remove reaction ash, residual fuel, and eroded particles to keep the plasma at a high quality level. At the same time, the divertor will dissipate about 15% of the total thermal power. In recently published helium-cooled divertor concepts [1,2] the plasma-facing structure consists of several hundred thousand single modules which may be roughly subdivided into four components: (1) a thermal shield made of tungsten which is brazed to, (2) a thimble of WL10 (W–1wt%La_2O_3) with an integrated, (3) cooling unit (e.g. pin or slot array, also made of tungsten or WL10) and (4) the underlying structure (He inlet, outlet, manifold, etc.) of ODS EUROFER.

In general, the problematic nature connected to divertor designs is the insufficient database on mechanical properties of refractory materials (especially tungsten and its alloys) which is obviously due to the fact that this material class has never been considered for structural components. Within the current divertor design this is mainly a concern of the thimble and its integrated cooling unit. Both are structural components where the most critical restrictions are prescribed by recrystallization and ductile-to-brittle transition temperatures. The former limits the upper and the latter the lower operating temperature. Clearly, recrystallization in structural

* Corresponding author. Tel.: +49 7247 82 2909; fax: +49 7247 82 4567.
E-mail address: michael.rieth@imf.fzk.de (M. Rieth).

0022-3115/$ - see front matter © 2005 Elsevier B.V. All rights reserved.
doi:10.1016/j.jnucmat.2005.03.013

components has to be avoided in any case, both, with respect to operation time as well as temperature. This leaves ductile-to-brittle transition temperature (DBTT) as the main focus for the design.

Unfortunately, there are no suitable DBTT data at all for tungsten and WL10. In the unirradiated, not recrystallized condition only tensile tests were performed, compilations are given in Refs. [3,4]. Also, irradiation-induced embrittlement was only characterized either by tensile tests [5,6] or by un-notched bend bars [7]. To our knowledge, indications on DBTT for unirradiated W and WL10 are only given in Ref. [4] to be in the range of 100–400 °C and in Ref. [3] (250–600 °C). Based on the assessment of these experiments and those with other refractory alloys [8], the operation temperature window for the current divertor design has been estimated to be in the range of 800–1200 °C [1].

Since it is well known, that DBTT strongly depends on the testing method, it is usually measured by standardized Charpy tests according to ASTM or ISO. Though DBTT cannot be directly used as design parameter like, for example, the lower operation temperature limit, Charpy tests on miniaturized specimens (either $3 \times 4 \times 27\ mm^3$ or $3.3 \times 3.3 \times 25.4\ mm^3$) have been established as *de facto* standard to characterize embrittlement of structural materials before and after irradiation. To our knowledge such experiments were never performed on tungsten or WL10 and probably not on tungsten alloys in general. Therefore, this paper focuses on new results achieved by high-temperature Charpy tests on commercially available tungsten and WL10. Furthermore, conclusions and impact on development and use of tungsten alloys for divertor applications are discussed.

2. Materials, microstructure and test procedure

Pure tungsten and WL10 rods (∅10 mm × 1000 mm, commercial standard products) have been purchased from Plansee Holding AG (Reutte, Austria). The final production steps were forging (hot work >80%), stress release heat treatment, and fine grinding of the surfaces. Main impurities are specified to be about 20 wt ppm Mo and 10 wt ppm Fe. The content of all other elements ranges well below 10 wt ppm.

The according microstructures are shown in Fig. 1. As can be clearly seen from the micrographs, both

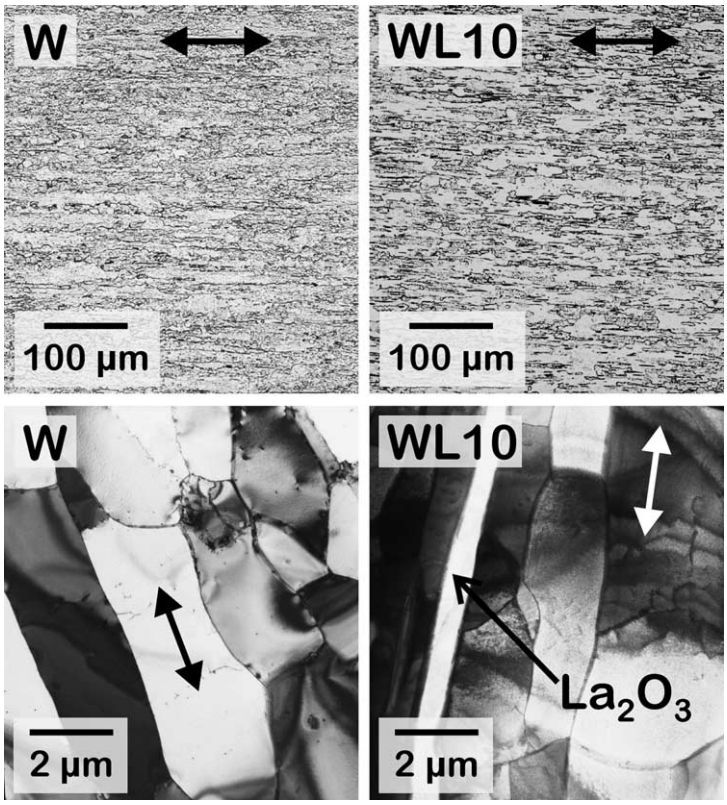

Fig. 1. Microstructure of the W and WL10 rod parallel to the rod axis (forging direction is indicated by double arrows). Upper row: optical micrographs. Lower row: TEM-micrographs.

grades show distinct forging textures. The TEM images prove further, that the grains are relatively inhomogeneous and elongated along the forging direction (rod axis) which is due to the high level of hot work. Therefore, the grain size can only be determined approximately and varies more or less around ASTM values of about 12–14. Also due to forging, the La_2O_3 particles are highly deformed to small needles with typical dimensions of about $\varnothing 0.4\ \mu m \times 20\ \mu m$. Vickers hardness for both materials averages out at HV30 = 455 ± 5.

From both rods, Charpy specimens ($3 \times 4 \times 27\ mm^3$, 60° notch, notch depth 1 mm, notch root radius 0.1 mm) were fabricated with the long side longitudinal and with the notch transversal to the rod axis (forging direction). That is, due to the above mentioned anisotropic microstructures, this orientation leads to optimum Charpy properties.

The Charpy tests were performed with a fully automatic testing device, i.e. specimens were moved from a stack into an electro furnace, heated to a specified temperature, transported to the support, centred and pushed on the support, and finally tested by the dropping 25 J pendulum. During testing, the specimen load was registered with a data acquisition rate of 300 kHz by strain gauges implemented in the hammer tup. The testing geometry was chosen according to the European standard EN 10 045 (tup radius 2 mm, support distance 22 mm, impact velocity 3.85 m/s). The heating and specimen transportation equipment allowed for testing temperatures up to 600 °C with an accuracy of minimum ±1% (specimen cooling during positioning included).

For test temperatures above 600 °C the specimens were manually positioned on the support and heated by different gas burners. With a butane/propane gas mixture the specimens could be heated to about 800 °C. But due to its size, the burner had to be removed before the pendulum was triggered. Therefore, the specimens cooled down to test temperatures of about 700 °C. Heating and cooling behaviour had been examined with specimens instrumented with an internal thermocouple. For even higher temperatures we used an acetylene-oxygen mixture with different gas flows (Fig. 2). With this procedure, test temperatures of 850–1050 °C could be achieved. Since the available acetylene burner was rather small, the specimen could be heated without interruptions, that is, the flame was permanently on – even during the tests. Again, the heating behaviour was examined with an instrumented specimen, and in addition, the whole procedure was recorded on video. Hence, the colour of the glowing specimen could be compared to the colour of the instrumented specimen to cross-check the accuracy of the according test temperature. To be on the sure side, we specify the accuracy to a rather conservative value of ±50 K.

Of course, objections might arise against such a brute tempering method with respect to oxidation and inhomogeneity of temperature distribution. But oxidation was observed only in a very thin surface layer (a lemon yellow WO_3 film) which obviously could not affect crack initiation and therefore, Charpy properties in general. As can be seen in Fig. 2, homogeneous temperature distributions were only reached in the area of the burner flame in a range of approximately 8 mm around the centre of the specimens. Due to the heat flow towards both specimens' ends (resting on the support) there certainly is a significant temperature drop. But again, the centre of the specimen is the relevant area where Charpy properties result by deformation, crack initiation, crack propagation, and fracture. Therefore, the test results should not be affected significantly by this kind of specimen heating.

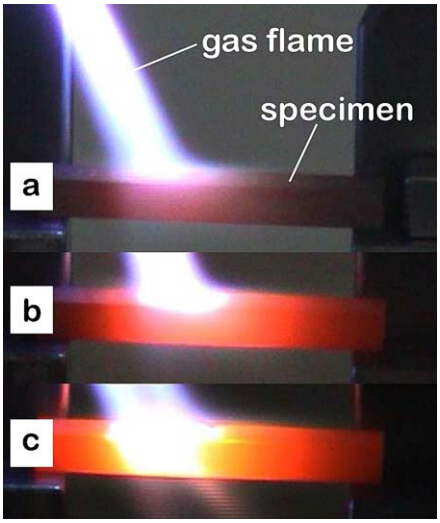

Fig. 2. Charpy specimens are heated to different temperatures with varying acetylene/oxygen gas flows. The brightness of the glowing specimens increases with temperature: (a) 850 °C, (b) 950 °C, (c) 1050 °C.

3. Results and evaluation

Evaluation of the instrumented Charpy test data has been performed according to EN ISO 14556. In addition, values for the yield strength have been determined by

$$\sigma_{yd} = C_g M_{bgy} / [B(W - a_0)^2] \quad (1)$$

with a constraint factor $C_g = 2.99$, specimen thickness $B = 3$ mm, specimen width $W = 4$ mm, notch depth $a_0 = 1$ mm. The bending moment M_{bgy} is calculated by

$$M_{bgy} = F_{gy} l / 4. \quad (2)$$

The according load at the yield limit F_{gy} has been extracted from the measured load–deflection curves and

the support span of the testing machine is $l = 22$ mm. Further details are given in [9,10]. The yield strength determined by Eqs. (1) and (2) is in good agreement with yield strength ($R_{p0.2}$) measured by tensile tests with maximum deviations of about 10%.

Brittle-to-ductile transitions by means of absorbed energy vs. test temperature plots are illustrated in Fig. 3 for tungsten, WL10, and a ferritic-martensitic 9Cr-1WVTa steel that is a typical reduced activation steel, similar to EUROFER and referred to, for example, in Ref. [11] as OPTIFER-Ia. Tungsten shows at 1050 °C no brittle fracture. Therefore, the upper-shelf energy (USE) can be assumed to be approximately 11.5 J which leads to a DBTT value of 800 ± 50 °C, determined at 0.5 USE as indicated in Fig. 3. The upper-shelf was not reached for WL10. Shear fractures could be clearly recognized even at 950 °C and 1050 °C. Furthermore, the energy difference of these two measurements indicates a broad scattering in the transition region which is typical for inhomogeneous materials. Hence, DBTT of WL10 may only be estimated. But a conservative DBTT estimate of 950 ± 50 °C would certainly be a realistic value (this estimate is based on the same USE as tungsten and uses the lowest energy values as illustrated in Fig. 3).

Load–deflection curves and fracture images are illustrated in Fig. 4, Table 1. For better evaluation the original oscillating load signals of the instrumented tub have been overlaid by average curves. Further, the slope of the elastic range has been drawn to the rising edge of the third oscillation which may be considered as yield limit.

What attracts immediate attention is that all fractures are not straight, i.e. crack propagation changed the direction during all Charpy tests – even in the most brittle states. A typical example is the tungsten specimen

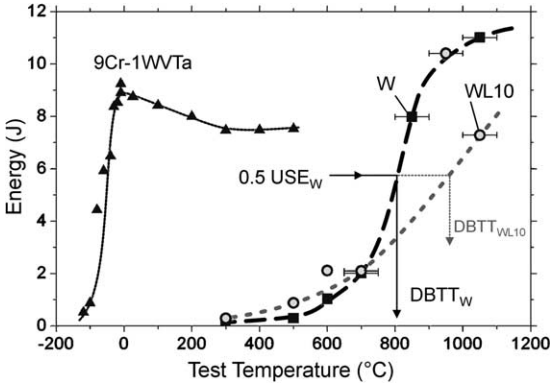

Fig. 3. Brittle-to-ductile transition of tungsten and WL10. Determination of DBTT at 0.5 USE leads to 800 ± 50 °C for tungsten while a conservative estimate for WL10 leads to DBTT of 950 ± 50 °C. For comparison, the transition of a 9Cr-1WVTa steel is also illustrated which clearly demonstrates the extraordinary brittleness of tungsten and WL10.

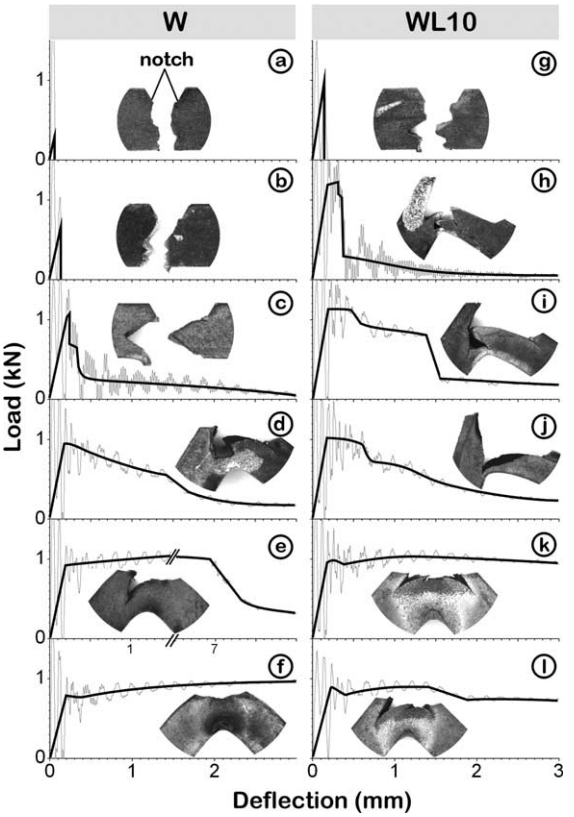

Fig. 4. Load–deflection curves and fracture images: (a–f) W, (g–l) WL10. The original oscillating load signals from the instrumented tup (thin lines) are overlaid by average load curves (thick lines). Test temperatures and results are given in Table 1.

Table 1
Materials, test temperatures, results

Fig. 4	Material	Temperature (°C)	Energy (J)	Yield strength (MPa)
(a)	W	300	0.18	–
(b)	W	500	0.29	–
(c)	W	600	1.03	670
(d)	W	700 ± 50	2.01	579
(e)	W	850 ± 50	7.98	548
(f)	W	1050 ± 50	11.01	475
(g)	WL10	300	0.28	–
(h)	WL10	500	0.88	731
(i)	WL10	600	2.11	682
(j)	WL10	700 ± 50	2.10	615
(k)	WL10	950 ± 50	10.41	585
(l)	WL10	1050 ± 50	7.28	548

tested at 600 °C (see Fig. 4(c)): first, the crack propagates at about 45° to the left and then it changes the direction to the right. This is reflected in the load curve by two consecutive rather steep signal drops. WL10

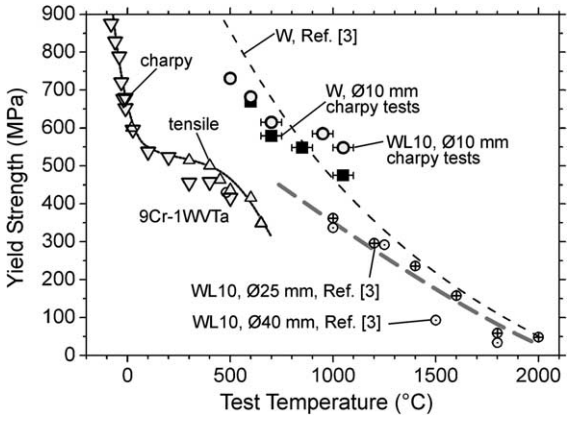

Fig. 5. Yield strength of tungsten, WL10, and 9Cr-1WVTa steel. Tensile test values of tungsten are only available as an average curve (short-dashed black line). The average yield strength of WL10 measured by tensile tests on two different rods is denoted by a long-dashed grey line. The agreement of yield strength values determined either by Charpy (downside triangles) or tensile (upside triangles) tests can be assessed from the results given for 9Cr-1WVTa steel (continuous black line).

shows a similar fracture behaviour. But in contrast to tungsten, here the cracks are propagating nearly perpendicular to the notch, that is, in forging direction. Such cracks appear in the load curves as moderate signal drops (see Fig. 4(i) and (j)).

Fully ductile fracture behaviour has been observed only for tungsten at 1050 °C (Fig. 4(f)). All other tests were accompanied by brittle fractures. In the most brittle state (Fig. 4(a), (b) and (g)), the specimens fractured immediately after touch by the tup (deflections of less than 0.2 mm), that is, in the elastic range.

Fig. 5 shows a comparison of yield strength values for tungsten, WL10, and 9Cr-1WVTa steel determined by Charpy tests as well as by tensile tests. Tensile results for W and WL10 have been extracted from Ref. [3]. Unfortunately, the tungsten yield strength is only given by an average curve. Yield strength values determined from tungsten Charpy tests vary around this average. Further, the WL10 Charpy test results show a slight tendency for higher yield. This is in contradiction to the yield values given in Ref. [3] which are clearly lower than the average tungsten yield strength.

4. Discussion

Evidently, the anisotropic grain distribution – due to the rod production process – is mirrored in the fracture appearance. Cracks propagate along the rod axis rather than in bending direction as usually observed during Charpy tests on homogeneous brittle materials. As could be seen from the micrographs (Fig. 1), La_2O_3 particles (which take about 3% of the total volume) are needle-shaped and oriented parallel to the forging direction within the WL10 rod. Therefore, Charpy specimens of this WL10 rod behave like uniaxial fibre-reinforced materials, that is, they preferably break open along the needles/fibres. This in turn, results in a further rise of DBTT compared to pure tungsten. The observed scattering in the transition region might also be due to the specific microstructure. Of course, scattering of the tungsten transition curve cannot be completely excluded based on these few Charpy tests.

DBTT values of 800 ± 50 °C for W and 950 ± 50 °C for WL10 seem to be rather high. But anyway, one has to take into account that the selected longitudinal specimens' orientation leads to the lowest possible transition temperatures. Different oriented specimens would therefore certainly yield DBTT values which are even higher.

WL10 is frequently categorized as dispersion strengthened tungsten and should show higher tensile and creep strength compared to pure tungsten. The former was already demonstrated on recrystallized W–0.8wt%La_2O_3 [12] while the latter has been verified recently with non-recrystallized WL10 at 1100 °C [13]. Therefore, the contradictorily yield data presented in Fig. 5 needs some interpretation. First of all, yield strength values of tungsten determined from our Charpy tests agree reasonably well with the average curve of Ref. [3]. Furthermore, the according values obtained for WL10 show a tendency for higher yield strength which would confirm the effect of dispersion strengthening. Therefore, the average curve may be accepted as rough clue, even though further information about experimental details is not given in Ref. [3]. But then the yield strength values for WL10 rods of diameter 25 mm and 40 mm – which are from the same production batch as the WL10 material we used for our investigations – do not fit in the picture, since they are significantly lower than the values for pure tungsten. Possible explanations could be either completely different microstructures or strain rate effects due to different testing parameters. It is also possible that the tensile specimens were produced and tested perpendicular to the forging direction. Unfortunately, neither Ref. [3] nor the original data sheets of the manufacturer show experimental details.

5. Conclusions

It is clear that for a full assessment of tungsten and its alloys for use as structural materials an according standard database of their mechanical properties had to be established first. But the results for pure tungsten and WL10 from standard Charpy tests are already rather disencouraging or, to be more specific, due to their high DBTT (and anisotropic microstructure as well) both

materials are not suitable as structural materials for divertor applications.

But then the question arises: is it possible at all to improve ductility of dispersion-strengthened tungsten? Of course, powder milling production without subsequent forging or rolling results in a homogeneous equiaxed grain distribution. Also the size of dispersion particles might be reduced and homogenized by mechanical alloying. But one can certainly not expect a significant improvement of DBTT by such treatments alone. Furthermore, the effect of dispersion strengthening tungsten is almost independent of the type of dispersoid. Be it La_2O_3 [12], CeO_2, ThO_2 [14], HfC [15], or TiC [16], all investigations led to improved creep or tensile strength, to higher recrystallization behaviour, and to better machining. On the other hand, a clear reduction of tensile elongation could be recognized. Also doping tungsten with Al–K–Si leads to comparable results [17], although based on a different mechanism. Only the addition of 0.2 wt% TiC was reported to improve DBTT [16] which should still be verified in standard tests.

In summary, Al–K–Si doping or dispersion strengthening tungsten may raise the recrystallization temperature significantly – and therefore the upper possible operating temperature of a structural component. In addition, creep and tensile strength might be improved. But for the use as structural material at lower operation temperatures around 800 °C and under fusion specific neutron irradiation, the material of consideration should exhibit DBTT of 200–400 °C measured by standard Charpy tests, at least in the unirradiated condition.

Since dispersion strengthening rather deteriorates the low temperature embrittlement, the focus should be laid on tungsten alloys. W–Re alloys, for example, show improved DBTT values with increasing amount of Re. But due to their high costs and difficult machining, W–Re alloys might be discarded for fusion applications. This would only leave the category of tungsten–heavy-metal alloys which are basically two-phase structures where the principal phase is nearly pure tungsten in association with a binder phase containing transition metals plus dissolved tungsten. Typical compositions of commercially available materials are, for example, W–3–5%Ni–1–2%Fe. In a divertor, the activation behaviour of such alloys would be comparable to EUROFER steel [18] and the mechanical properties [19] could probably be fitted to the needs of current divertor designs.

Acknowledgments

The authors would like to express their thanks to P. Graf and H. Zimmermann for preparing the LM-micrographs as well as to M. Klimiankou and U. Jäntsch for producing the TEM-images. This work was performed within the framework of the FUSION Project of Forschungszentrum Karlsruhe.

References

[1] P. Norajitra, L.V. Boccaccini, E. Diegele, V. Filatov, A. Gervash, R. Giniyatulin, S. Gordeev, V. Heinzel, G. Janeschitz, J. Konys, W. Krauss, R. Kruessmann, S. Malang, I. Mazul, A. Moeslang, C. Petersen, G. Reimann, M. Rieth, G. Rizzi, M. Rumyantsev, R. Ruprecht, V. Slobodtchouk, J. Nucl. Mater. 329–333 (2004) 1594.
[2] R. Kruessmann, P. Norajitra, L.V. Boccaccini, T. Chehtov, R. Giniyatulin, S. Gordeev, T. Ihli, G. Janeschitz, A.O. Komarov, W. Krauss, V. Kuznetsov, R. Lindau, I. Ovchinnikov, V. Piotter, M. Rieth, R. Ruprecht, V. Slobodtchouk, V.A. Smirnov, R. Sunyk, Forschungszentrum Karlsruhe, Report FZKA-6975, 2004.
[3] J.W. Davis, V.R. Barabash, A. Makhankov, L. Pöchl, K.T. Slattery, J. Nucl. Mater. 258–263 (1998) 308.
[4] I. Smid, M. Akiba, G. Vieider, L. Pöchl, J. Nucl. Mater. 258–263 (1998) 160.
[5] I.V. Gorynin, V.A. Ignatov, V.V. Rybin, S.A. Fabritsiev, V.A. Kazakov, V.P. Chakin, V.A. Tsykanov, V.R. Barabash, Y.G. Prokofyev, J. Nucl. Mater. 191–194 (1992) 421.
[6] J.M. Steinchen, J. Nucl. Mater. 60 (1976) 13.
[7] P. Krautwasser, H. Derz, E. Kny, High Temp. High Press. 22 (1976) 25.
[8] S.J. Zinkle, N.M. Ghoniem, Fus. Eng. Des. 51&52 (2000) 55.
[9] J.M. Alexander, T.J. Komoly, J. Mech. Phys. Solids 10 (1962) 265.
[10] W.L. Server, J. Test. Eval. JTEVA 6 (1978) 29.
[11] M. Rieth, B. Dafferner, H. Ries, O. Romer, Forschungszentrum Karlsruhe, Report FZKA-5550, 1995.
[12] M. Mabuchi, K. Okamoto, N. Saito, M. Nakanishi, Y. Yamada, T. Asahina, T. Igarashi, Mater. Sci. Eng. A 214 (1996) 174.
[13] M. Rieth, S. Heger, A. Falkenstein, Forschungszentrum Karlsruhe, IMF-I, private communication, Accepted for publication at the Annual Meeting on Nuclear Technology, Nuremberg, Germany, 10–12 May 2005.
[14] G.W. King, H.G. Sell, Trans. Met. Soc. AIME 233 (1965) 1104.
[15] W.D. Klopp, W.R. Witzke, J. Less-Common Met. 24 (1971) 427.
[16] Y. Kitsunai, H. Kurishita, H. Kayano, Y. Hiraoka, T. Igarashi, T. Takida, J. Nucl. Mater. 271&272 (1999) 423.
[17] P.K. Wright, Metall. Trans. A 9 (1978) 955.
[18] U. Fischer, Forschungszentrum Karlsruhe, IRS, private communication.
[19] F.A. Khalid, M.R. Bhatti, J. Mater. Eng. Perform. 8 (1999) 46.